Article

Cell Reports

Genomic and Epidemiological Surveillance of Zika Virus in the Amazon Region

Graphical Abstract

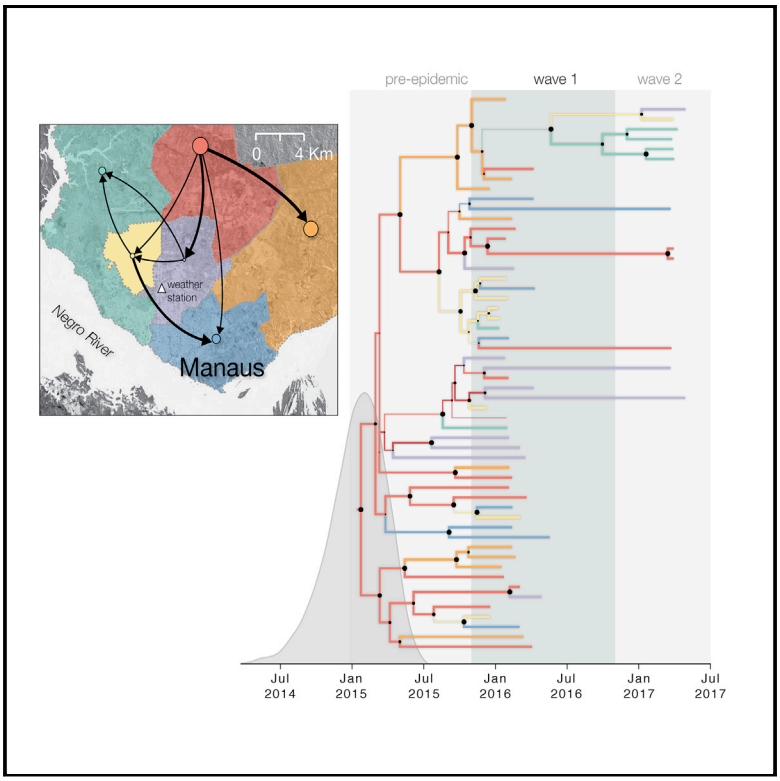

Authors

Marta Giovanetti, Nuno Rodrigues Faria, José Lourenço, ..., Felipe Gomes Naveca, Oliver G. Pybus, Luiz Carlos Alcantara

Correspondence

nuno.faria@zoo.ox.ac.uk (N.R.F.), oliver.pybus@zoo.ox.ac.uk (O.G.P.), luiz.alcantara@ioc.fiocruz.br (L.C.A.)

In Brief

Zika virus has caused an explosive epidemic linked to severe clinical outcomes in the Americas, but little is known about the epidemic in the Brazilian state of Amazonas. To gain insights into the routes of ZIKV introduction, Giovanetti et al. tracked the virus by sequencing genomes from infected patients from this region.

Highlights

- Epidemiological data reveal three ZIKV epidemic waves (2016, 2017, and 2018) in Manaus
- Our results suggest multiple introductions of ZIKV from northeastern Brazil to Manaus
- ZIKV cases in Manaus resulted from a single introduction event (January 2015)
- Spatial analysis suggested that northern neighborhoods acted as sources for transmission

Giovanetti et al., 2020, Cell Reports *30*, 2275–2283
February 18, 2020
https://doi.org/10.1016/j.celrep.2020.01.085

CellPress

Cell Reports
Article

Genomic and Epidemiological Surveillance of Zika Virus in the Amazon Region

Marta Giovanetti,[1,2,22] Nuno Rodrigues Faria,[2,3,22,*] José Lourenço,[3] Jaqueline Goes de Jesus,[1] Joilson Xavier,[2] Ingra Morales Claro,[4] Moritz U.G. Kraemer,[3] Vagner Fonseca,[2,5] Simon Dellicour,[6,7] Julien Thézé,[3] Flavia da Silva Salles,[4] Tiago Gräf,[8] Paola Paz Silveira,[8] Valdinete Alves do Nascimento,[9] Victor Costa de Souza,[9] Felipe Campos de Melo Iani,[2,10] Emerson Augusto Castilho-Martins,[11] Laura Nogueira Cruz,[12] Gabriel Wallau,[13] Allison Fabri,[1] Flávia Levy,[1] Joshua Quick,[14] Vasco de Azevedo,[2] Renato Santana Aguiar,[8] Tulio de Oliveira,[5] Camila Bôtto de Menezes,[15] Marcia da Costa Castilho,[16] Tirza Matos Terra,[17] Marineide Souza da Silva,[17] Ana Maria Bispo de Filippis,[1] André Luiz de Abreu,[12] Wanderson Kleber Oliveira,[18] Julio Croda,[19] Carlos F. Campelo de Albuquerque,[20] Marcio R.T. Nunes,[21] Ester Cerdeira Sabino,[4] Nicholas Loman,[14] Felipe Gomes Naveca,[9] Oliver G. Pybus,[3,*] and Luiz Carlos Alcantara[1,2,23,*]

[1]Laboratório de Flavivírus, Instituto Oswaldo Cruz Fiocruz, Rio de Janeiro, Brazil
[2]Laboratório de Genética Celular e Molecular, ICB, Universidade Federal de Minas Gerais, Belo Horizonte, Minas Gerais, Brazil
[3]Department of Zoology, University of Oxford, Oxford OX1 3PS, UK
[4]Instituto de Medicina Tropical, Universidade de São Paulo, São Paulo, Brazil
[5]KwaZulu-Natal Research Innovation and Sequencing Platform (KRISP), College of Health Sciences, University of KwaZuluNatal, Durban 4001, South Africa
[6]Spatial Epidemiology Lab, Université Libre de Bruxelles, Bruxelles, Belgium
[7]KU Leuven, Department of Microbiology and Immunology, Rega Institute, Laboratory for Clinical and Epidemiological Virology, Leuven, Belgium
[8]Instituto Gonçalo Moniz, Fundação Oswaldo Cruz, Salvador, Brazil
[9]Laboratório de Ecologia de Doenças Transmissíveis na Amazônia, Instituto Leônidas e Maria Deane, Fiocruz, Manaus, Brazil
[10]Laboratório Central de Saúde Pública, Fundação Ezequiel Dias, Belo Horizonte, Brazil
[11]Faculdade de Medicina, Universidade Federal do Amapá, Macapá, Brazil
[12]Coordenação Geral dos Laboratórios de Saúde Pública/Secretaria de Vigilância em Saúde, Ministério da Saúde (CGLAB/SVS-MS), Brasília, Distrito Federal, Brazil
[13]Fundação Oswaldo Cruz - Instituto Aggeu Magalhães, Recife, Pernambuco, Brazil
[14]Institute of Microbiology and Infection, University of Birmingham, Birmingham, UK
[15]Universidade do Estado do Amazonas, Manaus, Amazonas, Brazil
[16]Departamento de Virologia, Fundação de Medicina Tropical Doutor Heitor Vieira Dourado, Manaus, Amazonas, Brazil
[17]Laboratório Central de Saúde Pública do Amazonas, Manaus, Amazonas, Brazil
[18]Secretaria de Vigilância em Saúde, Ministério da Saúde (SVS-MS), Brasília, Distrito Federal, Brazil
[19]Departamento de Vigilância de Doenças Transmissíveis/Secretaria de Vigilância em Saúde, Ministério da Saúde (DEVIT/SVS-MS), Brasília, Distrito Federal, Brazil
[20]Organização Pan-Americana da Saúde/Organização Mundial da Saúde (OPAS/OMS), Brasília-DF, Brazil
[21]Center for Technological Innovations, Evandro Chagas Institute, Ministry of Health, Ananindeua, Pará, Brazil
[22]These authors contributed equally
[23]Lead Contact
*Correspondence: nuno.faria@zoo.ox.ac.uk (N.R.F.), oliver.pybus@zoo.ox.ac.uk (O.G.P.), luiz.alcantara@ioc.fiocruz.br (L.C.A.)
https://doi.org/10.1016/j.celrep.2020.01.085

SUMMARY

Zika virus (ZIKV) has caused an explosive epidemic linked to severe clinical outcomes in the Americas. As of June 2018, 4,929 ZIKV suspected infections and 46 congenital syndrome cases had been reported in Manaus, Amazonas, Brazil. Although Manaus is a key demographic hub in the Amazon region, little is known about the ZIKV epidemic there, in terms of both transmission and viral genetic diversity. Using portable virus genome sequencing, we generated 59 ZIKV genomes in Manaus. Phylogenetic analyses indicated multiple introductions of ZIKV from northeastern Brazil to Manaus. Spatial genomic analysis of virus movement among six areas in Manaus suggested that populous northern neighborhoods acted as sources of virus transmission to other neighborhoods. Our study revealed how the ZIKV epidemic was ignited and maintained within the largest urban metropolis in the Amazon. These results might contribute to improving the public health response to outbreaks in Brazil.

INTRODUCTION

Zika virus (ZIKV) is a flavivirus with an 11 kb positive-sense RNA genome that has caused an explosive epidemic in the Americas linked to severe congenital syndromes, including microcephaly (Petersen et al., 2016). ZIKV transmission occurs via the bite of infected *Aedes aegypti* mosquitoes, although sexual and vertical transmission, as well as transmission through blood transfusion, have been also reported (Petersen et al., 2016). Since the first detection of ZIKA in northeastern Brazil in May 2015 (Zanluca

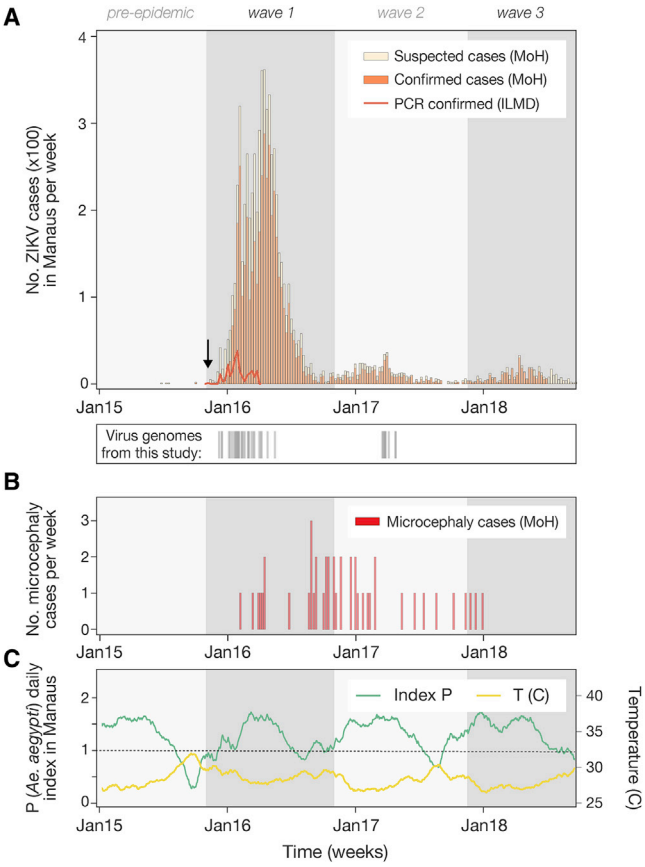

Figure 1. Zika Virus Transmission in Manaus

(A) ZIKV confirmed (dark orange bars) and suspected (light orange bars) cases per week in Manaus municipality notified from the Brazilian Ministry of Health (MoH), number of weekly RT-PCR-positive cases (red line) tested at Instituto Leonidas & Maria Deane (ILMD) FIOCRUZ, Amazonas, Brazil. Below, the dates of sample collection of the virus genomes generated in this study are shown using gray bars with transparency, such that darker shading reflects more dense sampling.

(B) Number of microcephaly cases per week in Manaus municipality notified to the Brazilian Ministry of Health.

(C) Daily transmission potential of *Aedes aegyti* in Manaus inferred using MVSE R-package (Obolski et al., 2019) from Manaus' climatic data. Relative humidity and temperature (degrees Celsius) were collected by an INMET weather station (for exact location, see Figure 7B).

et al., 2015; Campos et al., 2015), the country has reported nearly 1 million confirmed and suspected ZIKV infections, the greatest number among the 52 territories in the Americas that have reported ZIKV transmission (Pan American Health Organization, 2017; Zhang et al., 2017; Perkins et al., 2016). In recent years Brazil has been gripped by a wave of severe and overlapping epidemics of mosquito-borne viruses, which together have challenged passive syndromic surveillance and led to increased morbidity and disability (de Oliveira et al., 2017; Cao-Lormeau et al., 2016; Grubaugh et al., 2017). The northeastern and southeastern regions of Brazil have been severely hit by the ZIKV epidemic and account for 75% of reported ZIKV cases in Brazil between 2016 and 2018 (Secretaria de Vigilância em Saúde, Ministério da Saúde, 2018a; 2018b).

Although a smaller number of ZIKV infections have been reported in the northern region of Brazil encompassing the Amazon, several studies suggest that the region may be a location of entry for *Aedes*-borne viruses to Brazil, and increased epidemiological surveillance in the region is needed. For example, Brazilian dengue virus (DENV) and chikungunya virus (CHIKV) seem to have emerged first in the Amazon region before spreading to other, more densely populated locations (Nunes et al., 2012, 2014, 2015). The Amazon region is also home to a high diversity of mosquito-borne viruses (Vasconcelos et al., 1992), including Mayaro (Azevedo et al., 2009) and Oropouche (Azevedo et al., 2007), and an ecosystem that, under inadequate management, may facilitate the emergence and re-emergence of mosquito-borne virus epidemics (Faria et al., 2018; Vasconcelos, 2001). Moreover, climatic data suggest the possibility of year-round endemic transmission of arboviruses in the Amazon, which stands in contrast to seasonal epidemics in the southeastern, southern, and central western regions of Brazil (Messina et al., 2016; Obolski et al., 2019).

Between January 2015 and September 2018, Amazonas, the largest federal unit in Brazil, reported 4,929 Zika cases, including 46 cases of microcephaly in newborns. Most of these cases were reported in Manaus, the largest urban metropolis in the Amazon region, and cases were reported across several epidemic seasons (Secretaria de Vigilância em Saúde, Ministério da Saúde, 2019). However, the epidemic transmission and genomics of ZIKV in the Amazon region remain poorly understood. It is also unclear how and where Zika may have persisted in the Amazon region across epidemic seasons. Following our previous experience of using a mobile laboratory to investigate the genomic epidemiology of ZIKV in Brazil (Faria et al., 2016a), we used portable genome sequencing to locally generate ZIKV genomes from infected patients residing in Manaus. Samples were collected from febrile cases between December 2015 and April 2017. We use molecular epidemiology analysis to uncover the diversity and persistence of ZIKV in Manaus and its transmission in the Amazon region.

RESULTS

Expansion of the ZIKV Epidemic in Manaus

Up to September 2018, 6,987 ZIKV cases were reported by the main public health laboratory in Amazonas. The first PCR-confirmed case was identified in early November 2015 (Figure 1A, vertical arrow), and the first epidemic wave ("wave 1") peaked in mid-April 2016 (n = 288 cases/week) (Figure 1A). A second, smaller epidemic wave ("wave 2") peaked in early April 2017 (n = 32 cases/week) and was followed by a third epidemic wave ("wave 3") around mid-April 2018 (n = 30 cases/week). The estimated basic reproductive number of ZIKV from the first epidemic wave is $R_0 \sim 2.69$ (95% credible interval 2.32–3.11), in line with previous estimates (Faria et al., 2016b; Caminade et al., 2017).

Figure 1B shows the temporal distribution of microcephaly cases (n = 46) reported in Manaus between 2015 and 2018. To investigate the temporal association between confirmed cases of Zika and microcephaly cases in Manaus, we use a Poisson regression model that accounts for cross-correlation. We find evidence of a possible temporal association between the ZIKV

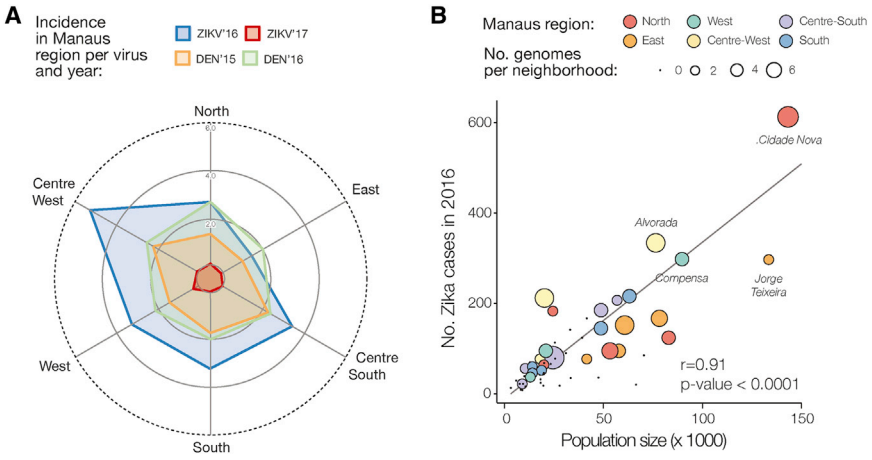

Figure 2. Spatial Incidence of Zika Virus in Manaus

(A) Circular plot shows ZIKV incidence (blue, 2016; red, 2017) and DENV incidence (orange, 2015; green, 2016) in the different areas of Manaus. The units for the incidence are cases per 1,000 inhabitants per year.

(B) Number of yearly ZIKV cases plotted against number of inhabitants per Manaus area (detailed data on ZIKV cases per neighborhood can be found in Table S3). The names of the four neighborhoods with the largest numbers of cases are shown. Circle sizes are proportional to the number of sequenced genomes per neighborhood, which are colored by region of Manaus.

See Table S2 for more details.

and microcephaly time series ($p < 0.001$, cross-correlation coefficient = 0.43, for December 19, 2015, to January 20, 2018). This model estimates that the microcephaly time series lags the ZIKV cases by 29 weeks in Manaus (Table S1).

To better understand the epidemic transmission of ZIKV in Manaus, we compiled climatic data from a weather station in Manaus city center and evaluated ZIKV transmission potential using the estimated suitability index *P* (Lourenço et al., 2017; Obolski et al., 2019). The estimated *P* index consistently reveals high suitability ($P > 1$) during the epidemic waves. According to the estimated *P* index, mosquitoes are able to contribute to transmission of ZIKV in Manaus throughout most of the year; that is, each year includes one or more long periods of time during which $P > 1$ (Figure 1C). The association between *P* and ZIKV cases was high (cross-correlation coefficient = 0.815, coefficient $p = 0.037$). Moreover, we estimate that ZIKV cases lag the *P* index time series by 4.7 weeks on average (Table S1).

Highest ZIKV Incidence in the Center-West Region of Manaus

We next explored the spatial distribution of ZIKV cases within individual neighborhoods of Manaus. Neighborhood-level yearly notified cases for ZIKV (2016 and 2017) and DENV (2015 and 2016) were made available from the Brazilian Ministry of Health, and case counts were grouped into six areas of Manaus city: north, west, east, center-west, center-south, and south (Figure 2). In 2016, ZIKV incidence in Manaus was highest in the center-west area (5.3 cases per 1,000 inhabitants); within this city area, the Dom Pedro neighborhood had the highest incidence (10.5 cases per 1,000 inhabitants; Table S2). The lowest incidence was recorded in the east area of Manaus (1.5 cases per 1,000 inhabitants). Incidence in all Manaus neighborhoods in 2017 was negligible (Figure 2A; Tables S2 and S3). As expected, ZIKV case numbers and neighborhood population size were strongly positively associated ($\rho = 0.91$, $p < 0.0001$; summarized in Figure 2B and detailed in Table S2), with 24% of ZIKV cases in Manaus being reported in the most populous north area of the city. We found a moderate association between ZIKV and DENV incidence per area in 2016 ($\rho = 0.47$, $p = 0.0002$), although DENV incidence was on average 1.4-fold lower in 2016 compared with that of ZIKV, possibly because of previous circulation of DENV and therefore accumulation of herd immunity to DENV (Figure 3).

Molecular Diagnostics and Genome Sequencing from Clinical Samples

A total of 525 samples from patients (68% woman [359 of 525]) visiting either local clinics or the main hospital in Manaus municipality between February 2014 and April 2017 were screened previously at Instituto Leonidas & Maria Deane (ILMD/FIOCRUZ) of Amazonas, the Central Laboratory of Public Health of Amazonas (LACEN-Amazonas), and the Flavivirus Laboratory at FIOCRUZ Rio de Janeiro (LABFLA/FIOCRUZ) using an in-house quantitative real time PCR assay targeting the ZIKV envelope gene region (Naveca et al., 2017). Of the tested samples, 218 (42%) tested positive for ZIKV, of which 158 (72.5%) were from female patients. For positive samples, PCR cycle threshold (Ct) values were on average 34.18 (range 15.19–41.01). We selected samples with Ct values of 38 or less for genome sequencing, resulting in 106 samples with an average Ct of 31.38 (range 15.19–38.00) (Table S4). These selected qRT-PCR-positive samples were obtained on average 3 days (range 0–14 days) after the onset of symptoms (Table S4) and were obtained from patients who resided in 40 different neighborhoods in Manaus. We used a MinION handheld nanopore sequencer to generate virus genome sequences from positive samples using our previously validated approach (Quick et al., 2017; Faria et al., 2017b). We successfully generated 59 complete and near complete genome sequences (average coverage 73%; see Figure 4; Table S5).

Genomic History of ZIKV in the Capital City of Amazonas State

To better understand the establishment and transmission of ZIKV in Manaus, we added our newly generated consensus genome sequences to a global dataset of 423 ZIKV genomes, including recently released ZIKV genomes from Angola and Cuba (Hill et al., 2019; Grubaugh et al., 2019), and we estimated an initial maximum likelihood (ML) phylogenetic tree (Figure 5). We find that 93% (55 of 59) of the novel Manaus isolates fall within a single large well-supported monophyletic clade (bootstrap score

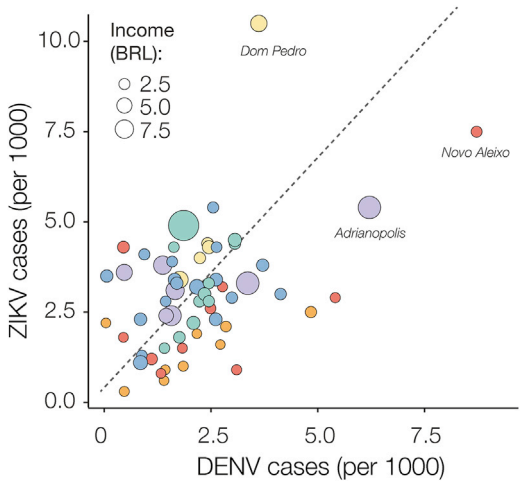

Figure 3. Number of Yearly ZIKV Cases Plotted against Number of DENV Cases per 1,000 Inhabitants per Year per Manaus Area

The names of the neighborhoods with largest numbers of cases are shown. Circle sizes are proportional to the number of sequenced genomes per neighborhood, which are colored by region of Manaus. Detailed data on ZIKV cases per neighborhood can be found in Table S3. See Table S2 for more details.

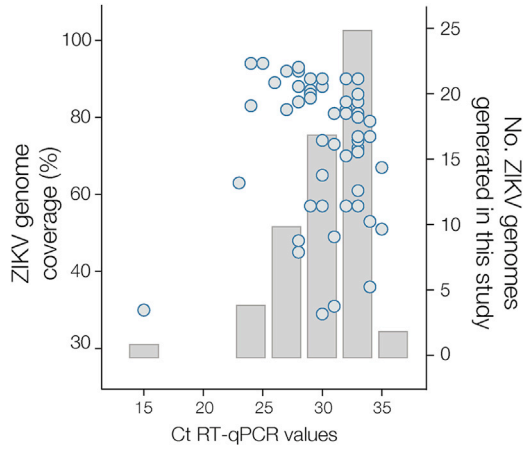

Figure 4. Zika Virus Sequencing Statistics

The percentage of ZIKV genome sequenced plotted against qRT-PCR Ct value for each sample (n = 59). Each circle represents a sequence recovered from an infected individual in Manaus.

[BS] = 94%) within the ZIKV American clade. This suggests that the ZIKV epidemic in Manaus was caused primarily by a single introduction, resulting in a large epidemic clade, named hereafter the Manaus clade.

We also identified four isolates from 2016 outside the main clade. Isolate AMA14, sampled in April 2016, falls basally to a clade containing six sequences from Chinese travelers infected in February 2016 in Venezuela (Sun et al., 2017) and a single sequence from the Dominican Republic. Isolate AMA59, sampled in January 2016, clusters with sequences from southeastern Brazil. A small clade containing isolates AMA53 and AMA20, sampled in January and April 2016, respectively, is closely related to a sequence from northeastern Brazil, and this resulting cluster is a sister clade to other sequences from the midwestern, southeastern, and northeastern regions of Brazil and also to three isolates from Angola (which likely derived from northeastern Brazil; Hill et al., 2019). Taken together these data suggest at least four independent introductions into Manaus. Although one isolate from Venezuela clusters together within the Manaus clade, we cannot make speculations about the transmission route between the two countries, because we do not have enough information about the epidemiological data of the sample, as well as a larger number of samples from Venezuela.

Spatiotemporal Evolution of ZIKV in Manaus

We estimated a timescale for the evolution of the Manaus clade using the best-fitting molecular clock model. A regression of genetic divergence from root to tip against sampling dates confirmed sufficient temporal signal (r^2 = 0.62) (Figure 6). The evolutionary rate of the Manaus clade was calculated to be 1.09×10^{-3} substitutions/site/year (s/s/y; 95% Bayesian credible interval [BCI] 7.7×10^{-4} to 1.43×10^{-3} s/s/y). This is in line with previous analyses of other ZIKV datasets from the Americas (Faria et al., 2016b, 2017b). We estimate the date of the most recent common ancestor (MRCA) of the ZIKV Manaus clade to be around January 2015 (95% BCI August 2014 to May 2015) (Figure 7A). Although this date represents a lower bound on the age of the Manaus clade, the estimated time of the MRCA of the Manaus clade coincides with a period of high ZIKV transmission potential in the city (Figure 1C).

In the Manaus clade, most of the sequences sampled from different city regions are interspersed, suggesting a highly interconnected dispersion pattern. We thus investigated the movement of ZIKV among geographic areas in Manaus using a discrete trait phylogenetic model. We find strong statistical support that the Manaus clade originated in the north area of the city (location posterior support = 0.92; Figure 7A). Our analysis identifies the north and east areas as probable source locations of ZIKV transmission in Manaus, seeding most of the virus lineage movement events within the city. The north and east are the most populated and least economically developed areas of Manaus, which suggests a possible link between ZIKV transmission and socioeconomic factors at a within-city level. ZIKV genome sequences from the center-south area were not phylogenetically clustered, indicating a lack of local virus transmission there. In contrast, six of ten strains from the west area of Manaus form a single monophyletic clade that resulted from an introduction during the peak of the epidemic in 2016 (Figures 1 and 7). These strains were isolated in April 2017, so this lineage may have circulated unnoticed for 10 months before detection.

We also estimated the contributions of different geographic areas of Manaus to the persistence of ZIKV in the city by estimating the waiting times between virus lineage movements (Markov rewards) across the phylogeny of the Manaus clade. Our results support the hypothesis that the north area of Manaus acts as the main source location (42% of the total branch duration in the time-scaled phylogeny is inferred to be located in the north area). Finally, we used our spatial analysis to infer the location in Manaus of ZIKV lineages that persisted across epidemic waves (Figure 1; see also Figure 7A). Our results suggest that ZIKV was

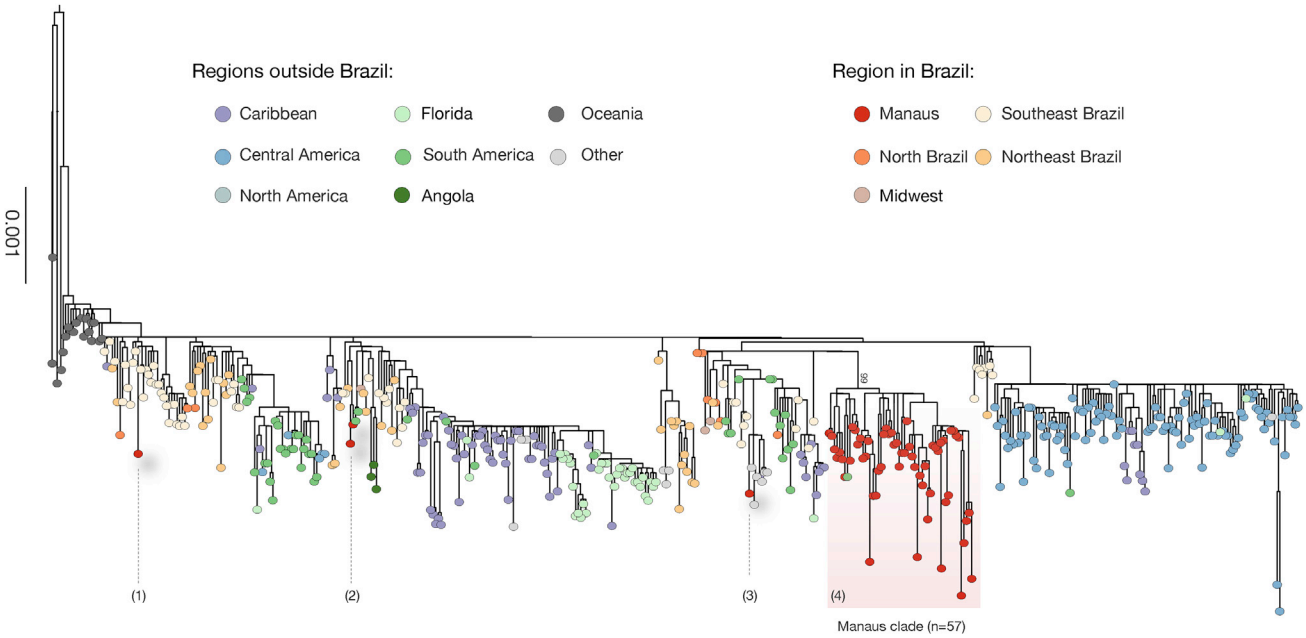

Figure 5. Maximum Likelihood Phylogeny of Zika Virus in the Americas

Maximum likelihood phylogeny was estimated with 482 complete or near complete genome sequences from Oceania and from the Americas. Sequences or clades from Manaus are numbered from 1 to 4, with the Manaus clade (4) being supported by a 94% bootstrap score. Colors represent different locations. Scale bar represents expected substitutions per nucleotide site.

able to persist locally across the 2015 and 2017 epidemic seasons in the north, east, south, and west areas of Manaus, which are also the four most populated areas of the city (Table S3).

DISCUSSION

In this study we characterized disease transmission in the large ZIKV outbreak in Manaus, Amazonas, in northern Brazil, using a combination of portable genome sequencing and epidemiological analysis. We find that the ZIKV epidemic in Manaus, the largest metropolis in the Amazon region, was ignited by an introduction of a single virus lineage, most likely from northeastern Brazil, which we infer was introduced around January 2015. This was a time of high climatic suitability for arbovirus transmission. We further show that the virus persisted locally until at least April 2017. Spatial genetic analysis indicates that the virus was introduced first to the northern neighborhoods of Manaus, from which the virus lineages seeded other nearby areas.

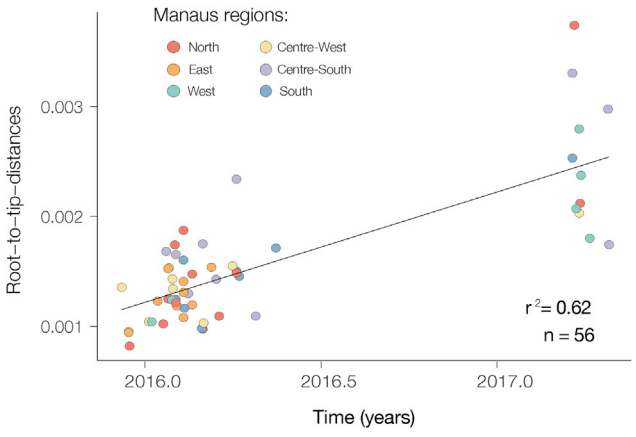

Figure 6. Root-to-Tip Plot

Regression of sequence sampling dates against root-to-tip genetic distances in a maximum likelihood phylogeny of the Manaus clade. Sequences are colored according to the six areas of Manaus (north, west, east, center-west, center-south, and south).

Analysis of the 59 ZIKV complete and partial genome sequences from 30 different neighborhoods in Manaus generated here provides a high-resolution contribution to our understanding of the introduction and progression of ZIKV in Brazil and to the transmission of ZIKV in tropical urban regions. Our analysis indicates that ZIKV was introduced to Manaus from the northeastern region of Brazil on at least four occasions. This agrees with our previous work that has found that northeastern Brazil played a significant role in the establishment and dissemination of ZIKV in the Americas (Faria et al., 2016b, 2017b).

Although evidence of cross-border transmissions among locations that share a tropical climate is frequent and has been observed previously in the region, for example, for DENV serotype 4 (Nunes, 2012) and CHIKV (Naveca et al., 2019), and although our results show that one isolate from Venezuela, a country with a high suitability for *Ae. aegypti* that has direct river connections to Manaus, clusters within the Manaus clade (Figure 5), we cannot exclude that some of the ZIKV introductions to Manaus were from Venezuela, therefore we cannot make speculations about the direction of the transmissions between

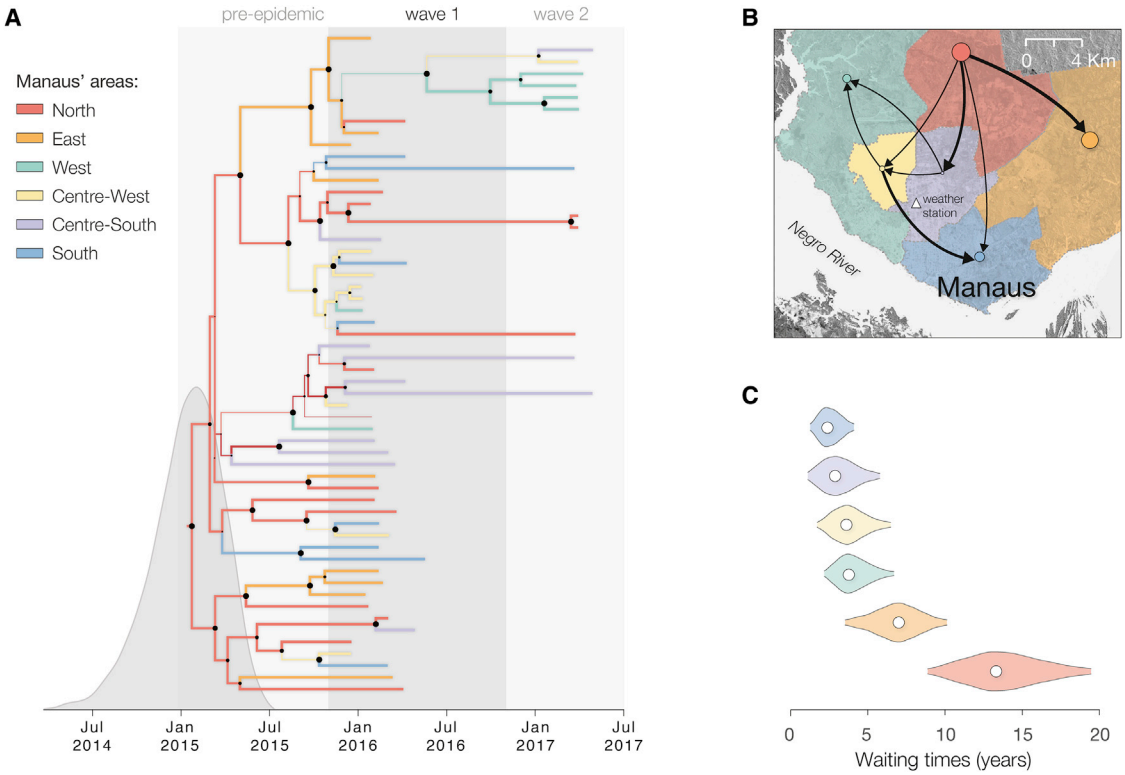

Figure 7. Phylogeography of ZIKV within Manaus

(A) Maximum clade credibility phylogeographic tree of the Manaus outbreak clade (n = 56). Branch colors represent most probable inferred locations. The black circles at internal nodes are sized in proportion to clade posterior probabilities. The branch thicknesses are sized in proportion to the most probable inferred locations.

(B) Map showing the inferred patterns of Zika virus transmission within areas of Manaus. Circles are proportional to the population size of each area of the city. The arrows are sized in proportion to the diffusion dispersal rate.

(C) Violin plot showing the posterior distribution of the total duration of phylogeny branches that are inferred to be located in each region of Manaus (Markov rewards). Colors represent different areas in Manaus as indicated in (A). The posterior distribution was calculated from 9,000 sampled trees.

the two countries, because of the lack of epidemiological data linked to this sample as well as a larger samples number from Venezuela.

Our within-city phylogeographic reconstruction is consistent with a gravity-like model of ZIKV dissemination, with virus transmission being driven by the most populated areas, which act as source locations, as shown previously for other infectious diseases (e.g., Kraemer et al., 2017, 2019a). The north area of Manaus has had the highest rate of population growth in recent years and has the second lowest income of all areas in the city. This suggests that demographic and socioeconomic factors have likely determined the incidence and persistence of the virus across Manaus neighborhoods (Lindoso and Lindoso, 2009; Hagan et al., 2016; Wilder-Smith et al., 2017). Our within-city phylogeographic reconstruction (Figure 7) further indicates that ZIKV transmission persisted through multiple epidemic waves in several neighborhoods.

It is important to note that phylogeographic analyses can be affected by sampling bias. In this study we compiled an updated dataset of ZIKV genome sequences dataset; comparatively few sequences from Brazil from 2017 and 2018 are available. This matches the small number of reported ZIKV cases in the country during this period, but undersampling may affect our conclusions concerning clustering with Manaus lineages after 2016. Regarding the within-city reconstructions, our sampling effort was successful in capturing ZIKV diversity in all main regions; the variation in sampling sizes obtained is approximately proportional to the number of ZIKV cases reported for each region in 2016 and 2017 (Table S3).

Epidemiological analysis of suspected ZIKV infections indicates a dominant epidemic wave of transmission in Manaus that peaked around mid-April 2016, followed by a second smaller wave in 2017. A third small epidemic peak in suspected cases can be noted around April 2018. We also find evidence that local microcephaly cases are correlated with local ZIKV cases and lag the latter by ~29 weeks. The introduction and spread of ZIKV over two or three consecutive waves in a given location has been observed previously and explained by the temporal accumulation of herd immunity (Lourenço et al., 2017; Ferguson et al., 2016). It has been reported also that the vast majority of Zika infections go unnoticed, and it is possible that the high similarity of case definitions for DENV, CHIKV, and ZIKV, which co-circulate in the Amazon region (Nunes et al., 2012, 2015; Vasconcelos et al., 1992; Naveca et al.,

2019; da Costa et al., 2018) could have resulted in a significant number of ZIKV infections being classified as either dengue or chikungunya at the beginning of the epidemic.

We find that local among-season ZIKV transmission in the Brazilian Amazon is consistent with sustained local year-round ecological suitability for *Aedes* spp., as previously predicted from climatic data alone (Bogoch et al., 2016), and also with the indication of a possible ZIKV persistence through natural vertical transmission in *Ae. aegypti* populations in Manaus (da Costa et al., 2018; Izquierdo-Suzán et al., 2019; Chaves et al., 2019), although these cases require more caution because the non-specific methodology used. Genetic and epidemiological analysis have indicated the northern region of Brazil has acted as a source region for DENV or as stepping-stone for the dissemination of arboviruses to other areas of the country (Faria et al., 2018) these trends may have been influenced by increases in human mobility and vector suitability (Kraemer et al., 2019b). Taken together, these results emphasize the ecological suitability of Manaus for the establishment of *Aedes*-borne viruses and highlight the need for continued arbovirus surveillance in Amazon urban areas.

In summary, we provide evidence for sustained local transmission of ZIKV in Manaus, Amazonas, between 2015 and 2017, and we reveal the epidemiological connections between Manaus and other locations in South America.

The spread of ZIKV in Manaus was mediated by climatic, socioeconomic, and demographic conditions, as well as by herd immunity (Lourenço et al., 2017), and our results shed light on the epidemiological dynamics of the virus urban tropical locations. Our work also provides an example of the relevance of integrating genetic and epidemiological surveillance when investigating arbovirus transmission (Kraemer et al., 2018). Ultimately such integration should aim for earlier detection of transmission of novel pathogens and for more real-time prediction of disease spread. The generation of genomic data by portable sequencing technology in local public health laboratories, as demonstrated here, can contribute substantially to these goals. Given the biodiversity of the Amazon basin, improving disease surveillance the region is crucial, both to improve public health responses and to increase our understanding of the diversity of known and unknown mosquito-borne viruses that co-circulate in the region.

STAR★METHODS

Detailed methods are provided in the online version of this paper and include the following:

- KEY RESOURCES TABLE
- LEAD CONTACT AND MATERIALS AVAILABILITY
- EXPERIMENTAL MODEL AND SUBJECT DETAILS
  - Sample collection
  - Ethical statement
- METHOD DETAILS
  - Nucleic acid isolation and RT-qPCR
  - cDNA synthesis and whole genome nanopore sequencing
  - Generation of consensus sequences
  - Collation of ZIKV complete genome datasets
  - Maximum likelihood analysis and clock signal estimation
  - Dated phylogenetics
  - Phylogeographic analysis
  - Epidemiological analysis
  - Temporal association between Zika virus and microcephaly cases
  - Daily Aedes-ZIKV transmission potential (P index)
- QUANTIFICATION AND STATISTICAL ANAYLSIS
  - Maximum Likelihood Phylogenetic Analysis
  - Dated phylogenetics and Phylogeographic analysis
  - Epidemiological analysis and Temporal association between Zika virus and microcephaly cases
  - Daily Aedes-ZIKV transmission potential (P index)
- DATA AND CODE AVAILABILITY
  - Data availability

SUPPLEMENTAL INFORMATION

Supplemental Information can be found online at https://doi.org/10.1016/j.celrep.2020.01.085.

ACKNOWLEDGMENTS

We thank Oxford Nanopore Technologies for technical support and QIAGEN for support of the ZIBRA-2 (Zika in Brazil Real Time Analyses-Second Round) project with reagents and equipment. This work was supported by Decit/SCTIE/MoH and CNPq (440685/2016-8 and 440856/2016-7); by CAPES (88887.130716/2016-00, 88881.130825/2016-00, and 88887.130823/2016-00); by the European Union (EU) Horizon 2020 Programme through ZIKAlliance (PRES-005-FEX-17-4-2-33); by the Medical Research Council and FAPESP CADDE partnership award (MR/S0195/1); and by the Oxford Martin School. N.R.F. is supported by a Sir Henry Dale Fellowship (204311/Z/16/Z). M.U.G.K. is supported by The Branco Weiss Fellowship - Society in Science, administered by ETH Zurich, and acknowledges funding from a Google Faculty Award and a Training Grant from the National Institute of Child Health and Human Development (T32HD040128). S.D. is supported by Fonds National de la Recherche Scientifique (FNRS; Belgium). The activities of the A.M.B.F. laboratory were supported by the Faperj under the grant no. E-26/2002.930/2016, by the International Development Research Centre (IDRC) Canada under the grant 108411-001) and the EU Horizon 2020 Programme through ZikaPlan and ZikAction (grants 734584 and 734857). M.G. is supported by Fundação de Amparo à Pesquisa do Estado do Rio de Janeiro (FAPERJ).

AUTHOR CONTRIBUTIONS

Conception and Design, M.G., N.R.F., N.L., O.G.P., and L.C.A. ; Investigations, M.G., N.R.F., F.G.N., J.G.J., J.X., I.M.C., F.S.S., P.P.S., V.A.N., V.C.S., F.C.M.I., G.W., E.A.C.-M., A.F., and F.L.; Data Curation, M.G., N.R.F., J.L., M.U.G.K., V.F., S.D., J.T., O.G.P., and L.C.J.A.; Formal Analysis, M.G., N.R.F., J.L., M.U.G.K., S.D., and L.P.; Writing – Original Draft Preparation, M.G., N.R.F., J.L., M.U.G.K., F.G.N., O.G.P., and L.C.J.A.; Revision, M.G., N.R.F., J.L., M.U.G.K., F.G.N., O.G.P., T.G., M.R.T.N., T.O., and L.C.J.A.; Resources, L.N.C., M.C.C., F.G.N., T.M.T., M.S.S., A.M.B.F., A.L.A., W.K.O., J.C., C.F.C.A., and L.C.J.A.

DECLARATION OF INTERESTS

The authors declare no competing interests.

Received: June 3, 2019
Revised: December 16, 2019
Accepted: January 24, 2020
Published: February 18, 2020

REFERENCES

Azevedo, R.S.S., Nunes, M.R.T., Chiang, J.O., Bensabath, G., Vasconcelos, H.B., Pinto, A.Y., Martins, L.C., Monteiro, H.A., Rodrigues, S.G., and Vasconcelos, P.F. (2007). Reemergence of Oropouche fever, northern Brazil. Emerg. Infect. Dis. *13*, 912–915.

Azevedo, R.S.S., Silva, E.V., Carvalho, V.L., Rodrigues, S.G., Nunes-Neto, J.P., Monteiro, H., Peixoto, V.S., Chiang, J.O., Nunes, M.R., and Vasconcelos, P.F. (2009). Mayaro fever virus, Brazilian Amazon. Emerg. Infect. Dis. *15*, 1830–1832.

Bogoch, I.I., Brady, O.J., Kraemer, M.U.G., German, M., Creatore, M.I., Kulkarni, M.A., Brownstein, J.S., Mekaru, S.R., Hay, S.I., Groot, E., et al. (2016). Anticipating the international spread of Zika virus from Brazil. Lancet *387*, 335–336.

Caminade, C., Turner, J., Metelmann, S., Hesson, J.C., Blagrove, M.S., Solomon, T., Morse, A.P., and Baylis, M. (2017). Global risk model for vector-borne transmission of Zika virus reveals the role of El Niño 2015. Proc. Natl. Acad. Sci. U S A *114*, 119–124.

Campos, G.S., Bandeira, A.C., and Sardi, S.I. (2015). Zika virus outbreak, Bahia, Brazil. Emerg. Infect. Dis. *21*, 1885–1886.

Cao-Lormeau, V.M., Blake, A., Mons, S., Lastère, S., Roche, C., Vanhomwegen, J., Dub, T., Baudouin, L., Teissier, A., Larre, P., et al. (2016). Guillain-Barré syndrome outbreak associated with Zika virus infection in French Polynesia: a case-control study. Lancet *387*, 1531–1539.

Chaves, B.A., Junior, A.B.V., Silveira, K.R.D., Paz, A.D.C., Vaz, E.B.D.C., Araujo, R.G.P., Rodrigues, N.B., Campolina, T.B., Orfano, A.D.S., Nacif-Pimenta, R., et al. (2019). Vertical transmission of Zika virus (Flaviviridae, Flavivirus) in Amazonian Aedes aegypti (Diptera: Culicidae) delays egg hatching and larval development of progeny. J. Med. Entomol. *56*, 1739–1744.

da Costa, C.F., da Silva, A.V., do Nascimento, V.A., de Souza, V.C., Monteiro, D.C.D.S., Terrazas, W.C.M., Dos Passos, R.A., Nascimento, S., Lima, J.B.P., and Naveca, F.G. (2018). Evidence of vertical transmission of Zika virus in field-collected eggs of Aedes aegypti in the Brazilian Amazon. PLoS Negl. Trop. Dis. *12*, e0006594.

Darriba, D., Taboada, G.L., Doallo, R., and Posada, D. (2012). jModelTest 2: more models, new heuristics and parallel computing. Nat. Methods *9*, 772–778.

de Oliveira, W.K., de França, G.V.A., Carmo, E.H., Duncan, B.B., de Souza Kuchenbecker, R., and Schmidt, M.I. (2017). Infection-related microcephaly after the 2015 and 2016 Zika virus outbreaks in Brazil: a surveillance-based analysis. Lancet *390*, 861–870.

Drummond, A.J., Ho, S.Y., Phillips, M.J., and Rambaut, A. (2006). Relaxed phylogenetics and dating with confidence. PLoS Biol. *4*, e88.

Faria, N.R., Sabino, E.C., Nunes, M.R.T., Alcantara, L.C.J., Loman, N.J., and Pybus, O.G. (2016a). Mobile real-time surveillance of Zika virus in Brazil. Genome Med. *8*, 97.

Faria, N.R., Azevedo, R.D.S.D.S., Kraemer, M.U.G., Souza, R., Cunha, M.S., Hill, S.C., Thézé, J., Bonsall, M.B., Bowden, T.A., Rissanen, I., et al. (2016b). Zika virus in the Americas: early epidemiological and genetic findings. Science *352*, 345–349.

Faria, N.R., da Costa, A.C., Lourenço, J., Loureiro, P., Lopes, M.E., Ribeiro, R., Alencar, C.S., Kraemer, M.U.G., Villabona-Arenas, C.J., Wu, C.H., et al.; NHLBI Recipient Epidemiology and Donor Evaluation Study-III (REDS-III) (2017a). Genomic and epidemiological characterisation of a dengue virus outbreak among blood donors in Brazil. Sci. Rep. *7*, 15216.

Faria, N.R., Quick, J., Claro, I.M., Thézé, J., de Jesus, J.G., Giovanetti, M., Kraemer, M.U.G., Hill, S.C., Black, A., da Costa, A.C., et al. (2017b). Establishment and cryptic transmission of Zika virus in Brazil and the Americas. Nature *546*, 406–410.

Faria, N.R., Kraemer, M.U.G., Hill, S.C., Goes de Jesus, J., Aguiar, R.S., Iani, F.C.M., Xavier, J., Quick, J., du Plessis, L., Dellicour, S., et al. (2018). Genomic and epidemiological monitoring of yellow fever virus transmission potential. Science *361*, 894–899.

Ferguson, N.M., Rodríguez-Barraquer, I., Dorigatti, I., Mier-Y-Teran-Romero, L., Laydon, D.J., and Cummings, D.A. (2016). Benefits and risks of the Sanofi-Pasteur dengue vaccine: modeling optimal deployment. Science *353*, 1033–1036.

Ferreira, M.A.R., and Suchard, M.A. (2008). Bayesian analysis of elapsed times in continuous-time Markov chains. Can. J. Stat. *78*, 355–368.

Fonseca, V., Libin, P.J.K., Theys, K., Faria, N.R., Nunes, M.R.T., Restovic, M.I., Freire, M., Giovanetti, M., Cuypers, L., Nowé, A., et al. (2019). A computational method for the identification of Dengue, Zika and Chikungunya virus species and genotypes. PLoS Negl. Trop. Dis. *213*, 72–131.

Gill, M.S., Lemey, P., Faria, N.R., Rambaut, A., Shapiro, B., and Suchard, M.A. (2013). Improving Bayesian population dynamics inference: a coalescent-based model for multiple loci. Mol. Biol. Evol. *30*, 713–724.

Grubaugh, N.D., Ladner, J.T., Kraemer, M.U.G., Dudas, G., Tan, A.L., Gangavarapu, K., Wiley, M.R., White, S., Thézé, J., Magnani, D.M., et al. (2017). Genomic epidemiology reveals multiple introductions of Zika virus into the United States. Nature *546*, 401–405.

Grubaugh, N.D., Saraf, S., Gangavarapu, K., Watts, A., Tan, A.L., Oidtman, R.J., Ladner, J.T., Oliveira, G., Matteson, N.L., Kraemer, M.U.G., et al.; GeoSentinel Surveillance Network (2019). Travel surveillance and genomics uncover a hidden Zika outbreak during the waning epidemic. Cell *178*, 1057–1071.e11.

Hagan, J.E., Moraga, P., Costa, F., Capian, N., Ribeiro, G.S., Wunder, E.A., Jr., Felzemburgh, R.D., Reis, R.B., Nery, N., Santana, F.S., et al. (2016). Spatiotemporal determinants of urban Leptospirosis Transmission: Four-Year prospective cohort study of slum residents in Brazil. PLoS Negl. Trop. Dis. *10*, e0004275.

Hasegawa, M., Kishino, H., and Yano, T. (1985). Dating of the human-ape splitting by a molecular clock of mitochondrial DNA. J. Mol. Evol. *22*, 160–174.

Hill, S.C., Vasconcelos, J., Neto, Z., Jandondo, D., Zé-Zé, L., Aguiar, R.S., Xavier, J., Thézé, J., Mirandela, M., Micolo Cândido, A.L., et al. (2019). Emergence of the Asian lineage of Zika virus in Angola: an outbreak investigation. Lancet Infect. Dis. *19*, 1138–1147.

Izquierdo-Suzán, M., Zárate, S., Torres-Flores, J., Correa-Morales, F., González-Acosta, C., Sevilla-Reyes, E.E., Lira, R., Alcaraz-Estrada, S.L., and Yocupicio-Monroy, M. (2019). Natural vertical transmission of Zika virus in larval Aedes aegypti populations, Morelos, Mexico. Emerg. Infect. Dis. *25*, 1477–1484.

Katoh, K., and Standley, D.M. (2013). MAFFT multiple sequence alignment software version 7: Improvements in performance and usability. Molecular Biology and Evolution *30*, 772–780.

Kraemer, M.U.G., Faria, N.R., Reiner, R.C., Jr., Golding, N., Nikolay, B., Stasse, S., Johansson, M.A., Salje, H., Faye, O., Wint, G.R.W., et al. (2017). Spread of yellow fever virus outbreak in Angola and the Democratic Republic of the Congo 2015-16: a modelling study. Lancet Infect. Dis. *17*, 330–338.

Kraemer, M.U.G., Cummings, D.A.T., Funk, S., Reiner, R.C., Faria, N.R., Pybus, O.G., and Cauchemez, S. (2018). Reconstruction and prediction of viral disease epidemics. Epidemiol. Infect. *4*, 1–7.

Kraemer, M.U.G., Golding, N., Bisanzio, D., Bhatt, S., Pigott, D.M., Ray, S.E., Brady, O.J., Brownstein, J.S., Faria, N.R., Cummings, D.A.T., et al. (2019a). Utilizing general human movement models to predict the spread of emerging infectious diseases in resource poor settings. Sci. Rep. *9*, 5151.

Kraemer, M.U.G., Reiner, R.C., Brady, O.J., Messina, J.P., Gilbert, M., Pigott, D.M., Yi, D., Johnson, K., Earl, L., and Marczak, L.B. (2019b). Past and future spread of the arbovirus vectors Aedes aegypti and Aedes albopictus. Nat. Microbiol. *4*, 854–863.

Lanciotti, R.S., Kosoy, O.L., Laven, J.J., Velez, J.O., Lambert, A.J., Johnson, A.J., Stanfield, S.M., and Duffy, M.R. (2008). Genetic and serologic properties of Zika virus associated with an epidemic, Yap State, Micronesia, 2007. Emerg. Infect. Dis. *14*, 1232–1239.

Lemey, P., Rambaut, A., Drummond, A.J., and Suchard, M.A. (2009). Bayesian phylogeography finds its roots. PLoS Comput. Biol. *5*, e1000520.

Lindoso, J.A., and Lindoso, A.A. (2009). Neglected tropical diseases in Brazil. Rev. Inst. Med. Trop. Sao Paulo *51*, 247–253.

Loman, N.J., and Quinlan, A.R. (2014). Poretools: a toolkit for analyzing nanopore sequence data. Bioinformatics *30*, 3399–3401.

Lourenço, J., Maia de Lima, M., Faria, N.R., Walker, A., Kraemer, M.U., Villabona-Arenas, C.J., Lambert, B., Marques de Cerqueira, E., Pybus, O.G., Alcantara, L.C., and Recker, M. (2017). Epidemiological and ecological determinants of Zika virus transmission in an urban setting. eLife *6*, 290–82.

Messina, J.P., Kraemer, M.U., Brady, O.J., Pigott, D.M., Shearer, F.M., Weiss, D.J., Golding, N., Ruktanonchai, C.W., Gething, P.W., Cohn, E., et al. (2016). Mapping global environmental suitability for Zika virus. eLife *5*, 5–18.

Naveca, F.G., Nascimento, V.A.D., Souza, V.C., Nunes, B.T.D., Rodrigues, D.S.G., and Vasconcelos, P.F.D.C. (2017). Multiplexed reverse transcription real-time polymerase chain reaction for simultaneous detection of Mayaro, Oropouche, and Oropouche-like viruses. Mem. Inst. Oswaldo Cruz *112*, 510–513.

Naveca, F.G., Claro, I., Giovanetti, M., de Jesus, J.G., Xavier, J., Iani, F.C.M., do Nascimento, V.A., de Souza, V.C., Silveira, P.P., Lourenço, J., et al. (2019). Genomic, epidemiological and digital surveillance of Chikungunya virus in the Brazilian Amazon. PLoS Negl. Trop. Dis. *13*, e0007065.

Nunes, M.R., Faria, N.R., Vasconcelos, H.B., Medeiros, D.B., Silva de Lima, C.P., Carvalho, V.L., Pinto da Silva, E.V., Cardoso, J.F., Sousa, E.C., Jr., Nunes, K.N., et al. (2012). Phylogeography of dengue virus serotype 4, Brazil, 2010-2011. Emerg. Infect. Dis. *18*, 1858–1864.

Nunes, M.R., Palacios, G., Faria, N.R., Sousa, E.C., Jr., Pantoja, J.A., Rodrigues, S.G., Carvalho, V.L., Medeiros, D.B., Savji, N., Baele, G., et al. (2014). Air travel is associated with intracontinental spread of dengue virus serotypes 1-3 in Brazil. PLoS Negl. Trop. Dis. *8*, e2769.

Nunes, M., et al. (2012). Phylogeography of dengue virus serotype 4, Brazil, 2010-2011. Emerg. Infect. Dis. *18*, 1858–1864.

Nunes, M.R.T., Faria, N.R., de Vasconcelos, J.M., Golding, N., Kraemer, M.U., de Oliveira, L.F., Azevedo, Rdo.S., da Silva, D.E., da Silva, E.V., da Silva, S.P., et al. (2015). Emergence and potential for spread of chikungunya virus in Brazil. BMC Med. *13*, 102.

Obolski, U., Perez, P.N., Villabona-Arenas, C.J., Thézé, J., Faria, N.R., and Lourenço, J. (2019). MVSE: an R-package that estimates a climate-driven mosquito-borne viral suitability index. Methods Ecol. Evol. *10*, 1357–1370.

Pan American Health Organization (2017).www.paho.org.

Perez-Guzman, P.N., Carlos Junior Alcantara, L., Obolski, U., de Lima, M.M., Ashley, E.A., Smithuis, F., Horby, P., Maude, R.J., Lin, Z., Kyaw, A.M.M., and Lourenço, J. (2018). Measuring mosquito-borne viral suitability in Myanmar and implications for local Zika virus transmission. PLoS Curr. *10*, 16–37.

Perkins, T.A., Siraj, A.S., Ruktanonchai, C.W., Kraemer, M.U., and Tatem, A.J. (2016). Model-based projections of Zika virus infections in childbearing women in the Americas. Nat. Microbiol. *1*, 16126.

Petersen, L.R., Jamieson, D.J., and Honein, M.A. (2016). Zika Virus. N. Engl. J. Med. *375*, 294–295.

Quick, J., Grubaugh, N.D., Pullan, S.T., Claro, I.M., Smith, A.D., Gangavarapu, K., Oliveira, G., Robles-Sikisaka, R., Rogers, T.F., Beutler, N.A., et al. (2017). Multiplex PCR method for MinION and Illumina sequencing of Zika and other virus genomes directly from clinical samples. Nat. Protoc. *12*, 1261–1276.

Rambaut, A., Lam, T.T., Max Carvalho, L., and Pybus, O.G. (2016). Exploring the temporal structure of heterochronous sequences using TempEst (formerly Path-O-Gen). Virus Evol. *2*, vew007.

Rambaut, A., Drummond, A.J., Xie, D., Baele, G., and Suchard, M.A. (2018). Posterior summarisation in Bayesian phylogenetics using Tracer 1.7. Syst. Biol. *67*, 901–904.

Secretaria de Vigilância em Saúde, Ministério da Saúde (2018a). Monitoramento dos casos de dengue, febre de chikungunya e doença aguda pelo vírus Zika até a semana epidemiológica 45 de 2018. Boletim Epidemiológico *49* (*53*). http://portalarquivos2.saude.gov.br/images/pdf/2018/novembro/29/BE-2018-58-SE-45.pdf.

Secretaria de Vigilância em Saúde, Ministério da Saúde (2018b). Monitoramento dos casos de dengue, febre de chikungunya e febre pelo vírus Zika até a semana epidemiológica 52, 2017. Boletim Epidemiológico *49* (*2*). http://portalarquivos2.saude.gov.br/images/pdf/2018/janeiro/23/Boletim-2018-001-Dengue.pdf.

Secretaria de Vigilância em Saúde, Ministério da Saúde (2019). Síndrome congênita associada à infecção pelo vírus Zika: situação epidemiológica, ações desenvolvidas e desafios de 2015 a 2019. Boletim Epidemiológico. http://portalarquivos2.saude.gov.br/images/pdf/2019/dezembro/05/be-sindrome-congenita-vfinal.pdf.

Shapiro, B., Rambaut, A., and Drummond, A.J. (2006). Choosing appropriate substitution models for the phylogenetic analysis of protein-coding sequences. Mol. Biol. Evol. *23*, 7–9.

Stamatakis, A. (2014). RAxML version 8: a tool for phylogenetic analysis and post-analysis of large phylogenies. Bioinformatics *30*, 1312–1313.

Suchard, M.A., Lemey, P., Baele, G., Ayres, D.L., Drummond, A.J., and Rambaut, A. (2018). Bayesian phylogenetic and phylodynamic data integration using BEAST 1.10. Virus Evol. *4*, vey016.

Sun, J., Wu, D., Zhong, H., Guan, D., Zhang, H., Tan, Q., Zhou, H., Zhang, M., Ning, D., Zhang, B., et al. (2017). Returning ex-patriot Chinese to Guangdong, China, increase the risk for local transmission of Zika virus. J. Infect. *75*, 356–367.

Thézé, J., Li, T., du Plessis, L., Bouquet, J., Kraemer, M.U.G., Somasekar, S., Yu, G., de Cesare, M., Balmaseda, A., Kuan, G., et al. (2018). Genomic epidemiology reconstructs the introduction and spread of Zika virus in Central America and Mexico. Cell Host Microbe *23*, 855–864.e7.

Vasconcelos, L. (2001). New forums out of sustainability—recent trends at local level. Proceedings of the First World Planning Congress – ACSP-AESOP-APSA-ANZAPS *32*, 11–15.

Vasconcelos, P.F.C., Travassos Da Rosa, A.P.A., Dégallier, N., Travassos Da Rosa, J.F.S., and Pinheiro, F.P. (1992). Clinical and ecoepidemiological situation of human arboviruses in Brazilian Amazonia. J. Brazil. Assoc. Adv. Sc. *44*, 117–124.

Wickham, H. (2016). In: Elegant Graphics for Data Analysis (New York: Springer-Verlag).

Wilder-Smith, A., Gubler, D.J., Weaver, S.C., Monath, T.P., Heymann, D.L., and Scott, T.W. (2017). Epidemic arboviral diseases: priorities for research and public health. Lancet Infect. Dis. *17*, e101–e106.

Yu, G., Tsan-Yuk Lam, T., Zhu, H., and Guan, Y. (2018). Two Methods for Mapping and Visualizing Associated Data on Phylogeny Using Ggtree. Biology and Evolution *35*, 3041–3043.

Zanluca, C., Melo, V.C., Mosimann, A.L., Santos, G.I., Santos, C.N., and Luz, K. (2015). First report of autochthonous transmission of Zika virus in Brazil. Mem. Inst. Oswaldo Cruz *110*, 569–572.

Zhang, Q., Sun, K., Chinazzi, M., Pastore Y Piontti, A., Dean, N.E., Rojas, D.P., Merler, S., Mistry, D., Poletti, P., Rossi, L., et al. (2017). Spread of Zika virus in the Americas. Proc. Natl. Acad. Sci. U S A *114*, E4334–E4343.

STAR★METHODS

KEY RESOURCES TABLE

REAGENT or RESOURCE	SOURCE	IDENTIFIER
Virus strains		
Zika Virus strains from Amazon	This Study	N/A
Biological Samples		
Serum, urine, cerebrospinal fluid samples from patients visiting either local clinics or the main hospital in Manaus municipality of Amazonas state	Amazonas State - Instituto Leonidas & Maria Deane (ILMD/FIOCRUZ) of Amazonas - The Central Laboratory of Public Health of Amazonas (LACEN-Amazonas) - The Flavivirus Laboratory at FIOCRUZ Rio de Janeiro (LABFLA/FIOCRUZ)	N/A
Critical Commercial Assays		
QIAamp Viral RNA Mini Kit	QIAGEN	Cat # 204443
TaqMan Fast Virus 1-Step Master Mix	Thermo-Fisher Scientific	Cat # 4444436
ProtoScript® II First Strand cDNA Synthesis Kit	New England Biolabs	Cat # E6560L
Q5 High-Fidelity DNA polymerase	New England Biolabs	Cat # M0491L
Agencourt AMPure XP	Beckman Coulter	Cat # A63880
Qubit dsDNA HS Assay Kit	QIAGEN	Cat # Q32851
CDC monoplex assay	Lanciotti et al., 2008	N/A
Native Barcoding Expansion 1-12 (PCR-free)	Oxford Nanopore Technologies	Cat # EXP-NBD104
DNA Sequencing Kit SQK-MAP007/ SQK-LSK108	Oxford Nanopore Technologies	Cat # SQK-LSK108
R9.4 flowcell	Oxford Nanopore Technologies	Cat # FLO-MIN106
Deposited Data		
59 Zika virus sequences 59 from Manaus, Amazonas State, Brazil have been deposited in the National Center for Biotechnology Information (NCBI) GenBank	This Study	National Center for Biotechnology Information (NCBI) GenBank: MK216687-MK216688; MK216690-MK216738; MK216740-MK216745; MK216747- MK216748.
423 publicly available Zika virus sequences obtained from the National Center for Biotechnology Information (NCBI) GenBank	N/A	National Center for Biotechnology Information (NCBI) GenBank: MK829154, MK829153, MK829152, MH544701, MH513600, MH513599, MH513598, MH157213, MH157208, MH157202, MH063265, MH063264, MH063263, MH063262, MH063261, MH063260, MH063259, MF783073, MF783072, MF073359, MF073358, MF073357, MG595216, MG494697, MF988743, KY441403, KY441402, KY441401, MF438286, MF384325, MF167360, MF159531, MF801426, MF801425, MF801424, KY606273, MF801423, MF801422, MF801421, MF801420, MF801419, MF801418, MF801417, KY606274, MF801416, MF801415, MF801414, MF801413, MF801412, MF801411, MF801410,

(*Continued on next page*)

Continued

REAGENT or RESOURCE	SOURCE	IDENTIFIER
		MF801409, MF801408, MF801407, MF801406, MF801405, MF801404,
		MF801403, MF801402, MF801401, MF801400, MF801399, MF801398,
		MF801397, MF801396, KY606272, MF801395, MF801394, KY606271,
		MF801393, MF801392, MF801391, MF801390, MF801389, MF801388,
		MF801387, MF801386, MF801385, MF801384, MF801383, MF801382,
		MF801381, MF801380, MF801379, MF801378, MF801377, MF434522,
		MF434521, MF434520, MF434519, MF434518, MF434517, MF434516,
		KX446950, KX446951, KX856011, KU870645, KY785416, KY014319,
		KY785471, KY014310, KY014311, KY014312, KY785418, KY785414,
		KY785444, KY785461, KY785442, KY014315, KY785452, KY014327,
		KY014306, KY785448, KY785458, KY785431, KY785421, KX421195,
		MF098770, MF098771, KY785454, KU501216, KU501217, KX262887,
		KX766029, KY120349, KY325465, KY328289, KY631493, KY693676,
		KY693677, KY765317, KY765318, KY765323, KY765324, KY765325,
		KY927808, KX520666, KX830930, KY785437, KY785436, KY014317,
		KY785446, KY785451, KY014320, KY014308, KY785410, KY014307,
		KY014309, KY785411, KY785427, KY785479, KY785480, KY785467,
		KY785425, KY785426, KY785409, KY014305, KY785469, KY014313,
		KY785423, KY785449, KY785463, KY785455, KY785417, KY785475,
		KY785465, KY785483, KY785433, KY785439, KY014303, KY014321,
		KY785415, KY014297, KY785450, KY014301, KY785429, KY785456,
		KY014296, KY014304, KY785420, KY785476, KY014300, KY014302,
		KY014318, KY785466, KY785485, KY785477, KY785441, KY785419,
		KY785428, KY014314, KY014295, KY785445, KY785412, KY785443,
		KY785457, KY014325, KY785440, KY785474, KY014298, KY014326,
		KY014316, KY014324, KY014322, KY014323, KX247646, KY014299,

(*Continued on next page*)

Continued

REAGENT or RESOURCE	SOURCE	IDENTIFIER
		KY785422, KY785472, KY785468, KY272991, KX156775, KX156774,
		KX156776, KU926309, MF098764, MF098765, MF098766, MF098769,
		MF098768, KX702400, KU926310, MF098767, KY785453, KY785478,
		KY785484, KY785473, KY785470, KY785460, KY785435, KY785434,
		KY785447, KY785413, KY785482, KY785424, KY785438, KY785430,
		KY785432, KY785481, KY785464, KY785462, KY785459, KX101065,
		KX101067, KX101064, KU940224, KU940227, KU940228, KX101063,
		KX101062, KX101061, KX101060, KX101066, KU312312, KU312313,
		KU312314, KU312315, KU501215, KU509998, KU646827, KU646828,
		KU647676, KU527068, KU707826, KU497555, KU729218, KU729217,
		KX197192, KU365780, KU365779, KU365778, KU365777, KX280026,
		KU321639, KU740184, KU758868, KU758869, KU758870, KU758871,
		KU758872, KU758873, KU758874, KU758875, KU758876, KU758877,
		KU761564, KU820897, KU820898, KU853012, KU922960, KU937936,
		KU955590, KU991811, KX051563, KX056898, KX087101, KX087102,
		KX197205, KX198135, KX212103, KX269878, KX377337, KX548902,
		KX601168, KX673530, KX766028, KX811222, KX879603, KX879604,
		KY003153, KY003154, KY003155, KY003156, KY003157, KY014328,
		KY014329, KY317936, KY317937, KY317938, KY317939, KY317940,
		KY348640, KY558989, KY558990, KY558991, KY558992, KY558993,
		KY558994, KY558995, KY558996, KY558997, KY558998, KY558999,
		KY559000, KY559001, KY559002, KY559003, KY559004, KY559005,
		KY559006, KY559007, KY559008, KY559009, KY559010, KY559011,
		KY559012, KY559013, KY559014, KY559015, KY559016, KY559017,
		KY559018, KY559019, KY559020, KY559021, KY559022, KY559023,
		KY559024, KY559025, KY559026, KY559027, KY559028, KY559029,

(*Continued on next page*)

Continued

REAGENT or RESOURCE	SOURCE	IDENTIFIER
		KY559030, KY559031, KY559032, KY631492, KY693678, KY693679,
		KY693680, KY817930, KY989971, KX447521, KX447520, KX447519,
		KX447518, KX447517, KX447516, KX447515, KX447514, KX447513,
		KX447512, KX447511, KX447510, KX447509, KX369547, KJ776791,
		KU681081, KU681082, JN860885, EU545988, KY075932, KX922706,
		KX922707, KX832731, KX838904, KX838905, KX838906, KX922708,
		KY075937, KY075938, KY075939, KY075933, KY317936, KY317937,
		KY317939, KY317940, KY317938, MF159531, MH063260, MH063261,
		MH063262, MH063263, KX842449, MH063264, MH063265, FL257|/H,
		KY075934, KX922703, KY075935, KX922704, KX922705, KY075936.
Oligonucleotides		
ZIKV 1086 5′-CCGCTGCCCAACACAAG-3′	Lanciotti et al., 2008	N/A
ZIKV 1162c 5′-CCACTAACGTTCTTTTGCAGACAT-3′	Lanciotti et al., 2008	N/A
ZIKV 1107-FAM 5′-AGCCTACCTTGACAAGCAGTCA GACACTCAA /3IABkFQ −3′	Lanciotti et al., 2008	N/A
Software and Algorithms		
BEAST	Suchard et al., 2018	http://beast.community
jModelTest2	Darriba et al., 2012	https://github.com/ddarriba/jmodeltest2
MAFFT	Katoh and Standley, 2013	https://mafft.cbrc.jp/alignment/server/
RAxML v8	Stamatakis, 2014	https://github.com/stamatak/standard-RAxML
Zika Virus Typing tool	Fonseca et al., 2019	http://www.krisp.org.za/tools.php
PrimalScheme	Quick et al., 2017	http://primal.zibraproject.org
QGIS	QGIS Development Team	https://qgis.org/en/site/
R Statistical Computing Software	The R Foundation	https://www.r-project.org/
R-package bdskytools	N/A	https://github.com/laduplessis/bdskytools
R-package ggplot2	Wickham, 2016	https://ggplot2.tidyverse.org
R-package ggtree	Yu et al., 2018	https://github.com/YuLab-SMU/ggtree
TempEst	Rambaut et al., 2016	http://beast.community/tempest
Tracer	Rambaut et al., 2018	http://beast.community/tracer
Albacore	Loman and Quinlan, 2014	https://github.com/nanoporetech
Nanopolish	Loman and Quinlan, 2014	https://github.com/jts/nanopolish
Porechop	Loman and Quinlan, 2014	https://github.com/rrwick/Porechop
Other		
Alignment used in phylogenetic analyses, including 196 publicly available Zika virus sequences and 59 Zika virus sequences generated in this study	This Study	N/A

LEAD CONTACT AND MATERIALS AVAILABILITY

Further information and requests for laboratory resources and reagents should be directed to and will be fulfilled by the corresponding author, Luiz Carlos Junior Alcantara (luiz.alcantara@ioc.fiocruz.br). Requests for computational resources and files should be

directed to and will be fulfilled by the corresponding authors, Oliver G. Pybus (oliver.pybus@zoo.ox.ac.uk) and Nuno Rodrigues Faria (nuno.faria@zoo.ox.ac.uk). This study did not generate new unique reagents.

EXPERIMENTAL MODEL AND SUBJECT DETAILS

Sample collection

Samples (serum, urine, cerebrospinal fluid) from patients visiting either local clinics or the main hospital in Manaus municipality of Amazonas state were collected for molecular diagnostics and sent for testing at IMLD/FIOCRUZ, LACEN-Amazonas and LABFLA/FIOCRUZ. Sampled individuals that were subjected to molecular diagnostics presented exanthema accompanied by two or more of the following symptoms: fever, headache, conjunctivitis, arthralgia, myalgia, and edema. The majority of samples were linked to a digital record that collated epidemiological and clinical data such as date of sample collection, municipality of residence, neighborhood of residence, demographic characteristics (age and sex) and date of onset of clinical symptoms (Tables S4 and S5).

Ethical statement

The project was supported by the Pan American World Health Organization (PAHO) and the Brazilian Ministry of Health (MoH) as part of the arboviral genomic surveillance efforts within the terms of Resolution 510/2016 of CONEP (Comissão Nacional de Ética em Pesquisa, Ministério da Saúde; National Ethical Committee for Research, Ministry of Health). The diagnostic of ZIKV infection at ILMD was approved by the Ethics Committee of the State University of Amazonas (CAAE: 56.745.116.6.0000.5016).

METHOD DETAILS

Nucleic acid isolation and RT-qPCR

Most of the Zika-suspected clinical samples were screened for ZIKV RNA from serum (86%), urine (3.5%) and cerebrospinal fluid (CSF) (11%). Samples were obtained from 0 to 31 days after the onset of symptoms. Viral RNA was isolated from 140 μl samples using the QIAamp Viral RNA Mini kit (QIAGEN, Hilden, Germany), according to the manufacturer's instructions. An internal positive control, the *Escherichia coli* bacteriophage MS2 (ATCC 15597-B1), was used during the RNA extraction as previously describe (Naveca et al., 2017). Cycle threshold (Ct) values were determined for all samples by probe-based reverse transcription quantitative real-time PCR (RT-qPCR) against the envelope (ENV) gene target for ZIKV detection (using 5′ FAM as the probe reporter dye) (Lanciotti et al., 2008) using the following primers 5′-CCGCTGCCCAACACAAG-3′ (forward) 5′-CCACTAACGTTCTTTTGCAGACAT. 3′ (reverse) and probe 5′- 6-FAM-AGCCTACCT/ZEN/TGACAAGCAGTCAGACACTCAA /3IABkFQ. RT-qPCR assays were performed with TaqMan Fast Virus 1-Step Master Mix in a reaction of 10 μL using a final concentration of 0.3 μM for primers and 0.1 μM for probe in a StepOnePlus Real-Time PCR System (Applied Biosystems) installed at the Real-Time PCR Platform of ILMD-FIOCRUZ.

cDNA synthesis and whole genome nanopore sequencing

DNA amplification and sequencing were attempted on the 106 selected RT-PCR positive samples that exhibited Ct-values < 38, in order to increase the genome coverage of clinical samples by nanopore sequencing (Quick et al., 2017). Extracted RNA was converted to cDNA using the Protoscript II First Strand cDNA synthesis Kit (New England Biolabs, Hitchin, UK) and random hexamer priming. Whole-genome amplification by multiplex PCR was attempted using the previously published Zika Asian primer scheme and 45 cycles of PCR using Q5 High-Fidelity DNA polymerase (NEB) as previously described (Quick et al., 2017). PCR products were cleaned-up using AmpureXP purification beads (Beckman Coulter, High Wycombe, UK) and quantified using fluorimetry with the Qubit dsDNA High Sensitivity assay on the Qubit 3.0 instrument (Life Technologies). PCR products for samples yielding sufficient material (more than 4ng/μL as determined using Qubit) were barcoded and pooled in an equimolar fashion using the Native Barcoding Kit (Oxford Nanopore Technologies, Oxford, UK). Sequencing libraries were generated from the barcoded products using the Genomic DNA Sequencing Kit SQK-MAP007/SQK-LSK208 (Oxford Nanopore Technologies) and were loaded onto a R9.4 flowcell. All sequencing was performed at ILMD-FIOCRUZ.

Generation of consensus sequences

Consensus sequences for each barcoded sample were generated following a previously published approach (Quick et al., 2017). Briefly, raw files were basecalled using Albacore (Loman and Quinlan, 2014), demultiplexed and trimmed using Porechop. Nanopolish variant calling was applied to the assembly to detect single nucleotide variants to the reference ZIKV genome (KJ776791). Only positions with ≥ 20x genome coverage were used to produce consensus alleles. Regions with lower coverage, and those in primer-binding regions were masked with N characters.

Collation of ZIKV complete genome datasets

Two complete or near-complete ZIKV genome datasets were generated. Dataset 1 (n = 482) comprised the data reported in this study (n = 59) plus a larger and updated dataset including recently released data from the ZIKV epidemic in Angola and Cuba (Hill et al., 2019; Grubaugh et al., 2019). Subsequently, to investigate the dynamic of the ZIKV infection within Manaus, genetic analyses

were conducted on a smaller dataset including only sequences pertaining to the largest clade of virus strains circulating in Manaus (n = 56).

Maximum likelihood analysis and clock signal estimation

Maximum likelihood (ML) trees were estimated using RAxML v8 (Stamatakis, 2014) under an HKY nucleotide substitution model (Hasegawa et al., 1985), with a gamma distribution of among site rate variation (HKY + G + I) as selected by jModeltest.v.2 (Darriba et al., 2012). Statistical robustness of tree topology was inspected using 1000 bootstrap replicates; a bootstrap value > 80% was considered notable. To estimate temporal signal in each dataset, sample collection dates were regressed against root-to-tip genetic distances obtained from the ML phylogenies using TempEst (Rambaut et al., 2016). When precise sampling dates were not available, a precision of 1 month or 1 year in the collection dates was considered.

Dated phylogenetics

To estimate time-calibrated phylogenies dated from time-stamped genome data, we conducted phylogenetic analysis using the Bayesian software package BEASTv.1.10.2 (Suchard et al., 2018). As previously (Thézé et al., 2018), we used the HKY nucleotide substitution model with codon partitions (Shapiro et al., 2006) and Bayesian Skygrid tree prior (Gill et al., 2013) with an uncorrelated relaxed clock with a lognormal distribution (Drummond et al., 2006). Analyses were run in duplicate in BEASTv.1.10.2 (Suchard et al., 2018) for 50 million MCMC steps, sampling parameters and trees every 5000th step. A non-informative continuous time Markov chain reference prior on the molecular clock rate was used (Ferreira and Suchard, 2008). Convergence of MCMC chains was checked using Tracer v.1.7.1 (Rambaut et al., 2018). Maximum clade credibility trees were summarized using TreeAnnotator after discarding 10% as burn-in.

Phylogeographic analysis

We investigated the dynamics of ZIKV infection and virus lineage movements in Manaus using a sampled set of time-scaled phylogenies and the sampling location (area in Manaus) of each geo-referenced ZIKV sequence, as shown in Table S6. We discretised sequence sampling locations by considering 6 distinct geographic areas of the Manaus city: north (n = 13), east (n = 9), south (n = 8), west (n = 6), central-west (n = 10), and center-south (n = 10), as shown in Figure 7. Phylogeographic reconstructions were conducted using the asymmetric discrete trait model implemented in BEASTv1.10.2 (Lemey et al., 2009). As part of the flexible discrete trait phylogeographic approach implemented in BEASTv1.10.2, we also estimated posterior expectations both the number of transitions among areas (Markov jumps) and the waiting times between transitions (Markov rewards) (Gill et al., 2013). Maximum clade credibility trees were summarized using TreeAnnotator after discarding 10% as burn-in. While the sampling is relatively homogeneous among sampled locations, the phylogeographic reconstruction will remain sampling dependent. For example, sampling effort could impact on the estimated transition frequencies among locations. However, with careful interpretation, phylogeographic analysis can provide valuable information about dispersal dynamics, including information about linkages that would not be evident without genomic data.

Epidemiological analysis

Number of weekly Zika virus cases in the municipality of Manaus were obtained from the Brazilian Ministry of Health. Cases were defined as suspected ZIKV infection when patients presented maculopapular rash and at least two of the following symptoms: fever, conjunctivitis, polyarthralgia or periarticular edema. Details and limitations of Zika virus surveillance approach based on notified or suspected cases have been described in more detail elsewhere (Faria et al., 2017b). The epidemic basic reproductive number, R_0, was estimated as previously described (Faria et al., 2017a). In brief, we fit a simple exponential growth rate model to weekly case counts from the first epidemic wave in Manaus. The period of exponential growth was selected, and a linear model was fitted to estimate the weekly exponential growth rate (r). We then derived reproductive number R_0 from r and a probability density distribution of the epidemic generation time. We assume a gamma-distribution function for the generation time with a mean of 20 days and a standard deviation of 7.4 days. We also explored other scenarios with generation time of 10 days.

Temporal association between Zika virus and microcephaly cases

The number of weekly microcephaly cases in the municipality of Manaus were obtained from the Brazilian Ministry of Health and are available. Zika virus and microcephaly case counts (n = 46) were compared using a Poisson regression model with Akaike Information Criteria to find the best-fitting time-lagged model. In this case, p value is the explanatory power of the Zika confirmed for microcephaly case counts to indicate the evidence for their association. Coefficients, cross-correlations and time-lags (in epidemiological weeks) for each comparison can be found in Table S1.

Daily Aedes-ZIKV transmission potential (P index)

Estimation of mosquito-borne virus suitability (P index) was calculated using a climate-driven method as previously described in (Obolski et al., 2019). The index P measures the reproductive (transmission) potential of an adult female mosquito for a given point in time. Manaus' average daily temperature and relative humidity (%) between 01/01/2014 to 21/01/2019 were obtained from the Instituto Nacional de Metereologia (INMET) weather station number 82331 (latitude: −3.11, longitude: −59.95). Climate data was

downloaded from INMET's website (http://www.inmet.gov.br/portal/). Moreover, for a comparison between the suitability index P and Zika confirmed cases, we considered Zika non-negative counts as continuous and applied a log(x+1) transformation. We focus on the epidemic season 14th November 2015 to 10th August 2016. An autoregressive integrated moving average (ARIMA) model was used to account for any residual autocorrelation (P). In this case, the p value reflects the explanatory power of suitability for Zika virus confirmed cases. We note that by using the index P as a proxy for transmission potential using climate data from a single weather station in Manaus, we do not take into account the possible effects of microclimate across the city. Although having been demonstrated to be highly correlated with mosquito-borne incidence in other cities of Brazil and elsewhere (Obolski et al., 2019; Perez-Guzman et al., 2018), the index P is not informed by factors that may play a role in transmission potential in Manaus, such as abundance of vegetation and human density or mobility.

QUANTIFICATION AND STATISTICAL ANAYLSIS

Maximum Likelihood Phylogenetic Analysis

To assess the suitability of substitution models for our ZIKV alignment we performed a statistical model selection procedure based on the Akaike information criterion, using jModelTest2 (Darriba et al., 2012). This identified the best fitting substitution model (HKY + G + I) for ML phylogenetic analysis. A phylogenetic bootstrap analysis with 100 replicates using RAxML v8 (Stamatakis, 2014) was conducted to evaluate the statistical support for nodes of the ML phylogeny.

Dated phylogenetics and Phylogeographic analysis

To assess whether our data was suitable for a molecular clock phylogenetic analysis, we evaluated the temporal evolutionary signal in our ZIKV alignment using the statistical approaches in TempEst (Rambaut et al., 2016). A linear regression between sample collection dates and root-to-tip genetic distances obtained from the ML phylogeny indicated that the feasibility of a molecular clock approach. A Bayesian MCMC approach implemented in BEAST v1.10.2 (Suchard et al., 2018) was used to infer molecular clock.

Epidemiological analysis and Temporal association between Zika virus and microcephaly cases

A linear regression model developed and described in Faria et al., (2017a), was used to assess the correlation between Zika virus and microcephaly cases, for each each distinct Manaus's neighborhoods.

Daily Aedes-ZIKV transmission potential (P index)

Estimation of mosquito-borne virus suitability (P index) was calculated using a climate-driven method as previously described in (Obolski et al., 2019). An autoregressive integrated moving average (ARIMA) model was used to account for any residual autocorrelation (P). This model measures the reproductive (transmission) potential of an adult female mosquito for a given point in time and explains the variation in the ZIKV transmission potential.

DATA AND CODE AVAILABILITY

Data availability

New sequences have been deposited in GenBank under accession numbers MK216687-MK216688; MK216690-MK216738; MK216740-MK216745; MK216747- MK216748.